

# Orientation effects on the melting of poly(ethylene terephthalate)

P. Nicholas, A. R. Lane and T. J. Carter

BICC Central Research Laboratory, 38 Ariel Way, Wood Lane, London W12 7DX, UK

and J. N. Hay

Chemistry Department, University of Birmingham, PO Box 363, Birmingham B15 2TT, UK

(Received 26 May 1987; revised 18 November 1987; accepted 24 November 1987)

Poly(ethylene terephthalate) (PET) is used as a loose tube sheathing material for glass optical fibres. It is important that the expansion coefficient of the tubing matches that of the glass fibre and hence the PET tubing is drawn to an amount calculated to give such equality. Extruded tubes of PET with draw ratios up to 5:1 have been examined by differential scanning calorimetry. Orientation progressively increases the temperature of onset of melting, but leaves the degree of crystallinity of the samples unaltered provided they are prepared under identical thermal treatments. Melting occurs over a narrower temperature range, and the height of the maximum specific-heat change during melting is a relative measure of the orientation. Samples with draw ratios above 3.5, which are difficult to distinguish by means of wide-angle X-ray diffraction measurements, can be distinguished by their melting points.

(Keywords: poly(ethylene terephthalate); draw ratio; melting; Hermans function; differential scanning calorimetry)

## INTRODUCTION

The properties of poly(ethylene terephthalate) (PET) are markedly dependent on thermal history, orientation and morphology. In particular, the degree of crystallinity and extent of physical ageing have pronounced effects on the impact behaviour<sup>1</sup>. Uniaxial orientation introduces an angular dependence to the properties, and adds further complexities to the measurement and definition of crystallinity.

The measurement of crystallinity in oriented PET depends on the method adopted and there is considerable confusion as to the structures present<sup>2</sup>. Prevorsek *et al.*<sup>3,4</sup>, from wide-angle X-ray diffraction (WAXD), predicted the presence of crystalline, amorphous and an intermediate mesomorphic phase. The proportions of the latter were determined from the intensities of the diffraction peaks from the (110), (010) and (100) planes. Others have discussed the concept of an oriented amorphous phase, and a random unoriented amorphous phase<sup>5-7</sup>. Each phase is an idealized model, and there will be regions of intermediate structure. However, each experimental technique makes a separate assessment of the relative abundance of the three phases, and gives a different measure of the degree of orientation and crystallinity.

Uniaxial orientation has a marked effect in raising the melting behaviour of polymers, and there has been some attempt to correlate this with morphology<sup>8</sup>.

The present paper deals with a study of orientation from its effect on the melting characteristics of drawn PET.

## EXPERIMENTAL

Commercial samples of PET, Arnite A06700 blended

0032-3861/88/050894-04\$03.00

© 1988 Butterworth & Co. (Publishers) Ltd.

894 POLYMER, 1988, Vol 29, May

with polyethylene (10%) obtained from Akzo, were used as drawn tubes. They were produced by extruding and stretching between differentially driven rollers. The ratio of the rotation speeds defined the draw ratio, i.e. the extensional ratio  $\lambda$ . Their processing conditions are listed in Table 1.

A Perkin-Elmer differential scanning calorimeter, model DSC-2C, was used with a controlled cooling accessory operating with liquid nitrogen, analogue-to-digital interface, 3600 data station and TADS thermal analysis software. Analyses were carried out under an atmosphere of nitrogen to prevent oxidative degradation, on 10 mg samples obtained by splitting the drawn tubes. Melting was examined from 450 to 550 K at heating rates of 10–80 K min<sup>-1</sup> correcting for thermal lag. The d.s.c.

Table 1 D.s.c. analysis of PET samples

Sample reference	Draw ratio, $\lambda$	Enthalpy of fusion (J g <sup>-1</sup> )	Peak height (cm)	Hermans function	Annealing temperature (K)
4A	2.5	42.2	7.2	0.61	498
5A	3.0	44.1	8.5	0.73	498
6A	3.5	44.9	9.3	0.77	498
7A	4.0	45.0, 45.1	8.5, 9.1	0.77	498
8A	4.5	45.5, 44.8	8.7, 8.8	0.78	498
9A	5.0	45.4	9.5	0.78	498
Heat cycled					
4B	1.0	42.5, 42.0	4.5, 4.9	—	— <sup>a</sup>
4B	2.5	41.1, 41.6	5.9, 5.8	—	—
5B	3.0	44.5, 44.4	8.2, 8.0	—	—
6B	3.5	46.5, 45.0	9.3, 9.7	—	—
7B	4.0	45.7, 45.4	9.0, 9.5	—	—
8B	4.5	45.6, 44.4	8.8, 7.2	—	—
9B	5.0	45.4, 44.8	8.7, 9.7	—	—

<sup>a</sup> Heat-cycled samples are unannealed

was calibrated with ultra-pure indium, assuming a heat of fusion of  $28.45 \text{ J g}^{-1}$ , and a melting point of  $429.78 \text{ K}$ .

X-ray diffraction measurements of crystalline preferred orientation were made using a Hilger and Watts Y144 diffractometer equipped with a specially designed tilting stage. Measurements followed the procedure of Dumbleton and Bowles<sup>9</sup>. This involved setting the diffractometer to receive diffracted radiation from the (105) crystal planes and then measuring variations of diffracted intensity as the sample was tilted over a  $180^\circ$  angular range. The (105) direction in the crystal lattice is located  $10^\circ$  away from the molecular chain direction and so the intensity distribution obtained consists of two superimposed peaks centred  $10^\circ$  either side of the sample axis. A computer peak-separation procedure has been used to resolve the profile into its two components, either of which represents the oriented distribution. From this the mean cosine function was calculated using the expression:

$$\langle \cos^2 \phi \rangle = \frac{\int I(\phi) \cos^2 \phi \sin \phi \, d\phi}{\int I(\phi) \sin \phi \, d\phi} \quad (1)$$

where  $\phi$  is the angle between the sample axis and the molecular chain direction. The Hermans function ( $f$ ) was then obtained from:

$$f = - (3 \langle \cos^2 \phi \rangle - 1) \quad (2)$$

In the assessment of preferred orientation in the samples, a number of simplifications are possible. First, the method of manufacture ensures that any orientation is uniaxial along the processing direction. Secondly, it is usual with uniaxially oriented polymers to assume that the only material feature that is likely to be oriented is the molecular chain direction. The orientation can then be described numerically by a series of Legendre polynomials. Most of the information is contained in the first term of this series, whose coefficient ( $P_2$ ) is equal to the Hermans function. The Hermans function alone was used to quantify the crystalline preferred orientation for the present series of samples, which differed in degree rather than type of orientation.

## RESULTS AND DISCUSSION

### Thermoanalytic analysis

D.s.c. was successful in distinguishing between the various experimental samples (see *Figure 1*).

(a) Undrawn extruded tube was amorphous, exhibiting a glass transition temperature at  $345 \text{ K}$  due to amorphous PET, a melting endotherm at  $390\text{--}400 \text{ K}$  due to the polyethylene phase, an exotherm at  $410 \text{ K}$  due to the crystallization of PET, and an endotherm due to melting at  $520 \text{ K}$ .

(b) On drawing, the PET crystallized and the glass transition and crystallization exotherms were no longer present in the thermogram. Annealed samples exhibited small endotherms about  $10 \text{ K}$  above their annealing temperature<sup>10</sup>, which was consistent with reorganization of the crystalline material. D.s.c. could be used to indicate the maximum crystallization temperature of commercial samples. Annealed samples were highly crystalline, at  $30\%$ .

WAXD studies were also consistent with the observations that PET tubing crystallized on drawing but

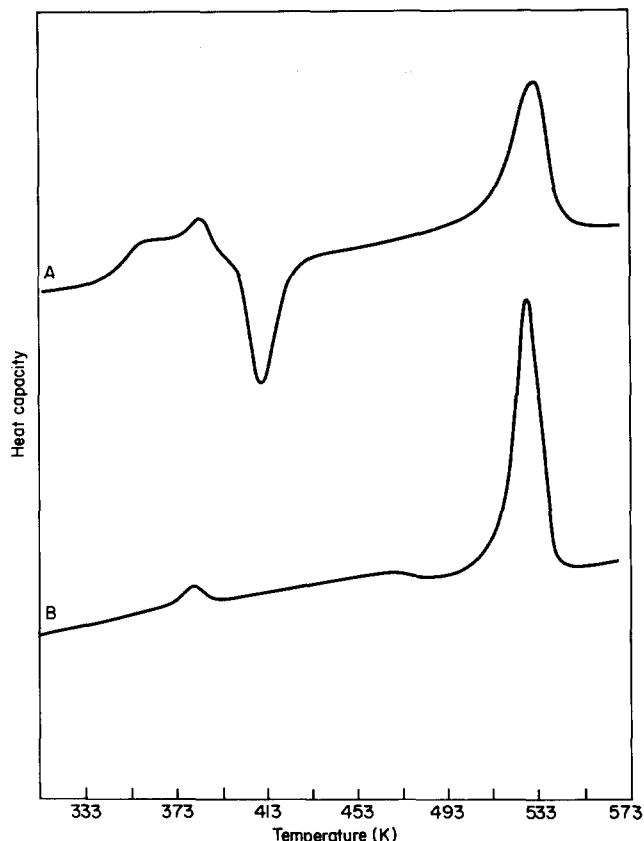


**Figure 1** D.s.c. heating scans on PET: A, unoriented; B, oriented and annealed at  $463 \text{ K}$

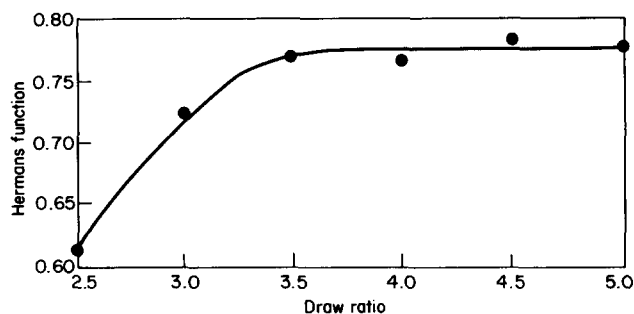


**Figure 2** The effect of draw ratio on the Hermans function for annealed samples 4A to 9A

the crystallites were ill-developed. Annealed specimens were highly crystalline and exhibited orientation in the PET domains only. The stretched polyethylene phase relaxed during annealing, and the intensities of the diffraction lines dropped to levels characteristic of unoriented material.

From the angular dependence of the X-ray diffraction plots, the Hermans function was calculated for the annealed specimens. It changed progressively with draw ratio  $\lambda$  up to values of  $3.5$  but became insensitive to values greater than this (see *Figure 2*).

D.s.c. measurement of the melting endotherm showed that the temperature range over which melting occurred was markedly dependent on the draw ratio (see *Figure 3*), and melting moved progressively to higher temperatures with increased draw ratios. The endotherms changed shape and melting occurred over a narrower temperature range. The extent to which this occurred, however, was dependent on the rate of heating and the effect reached a maximum at  $20 \text{ K min}^{-1}$  (see *Figure 4*). The nature of the

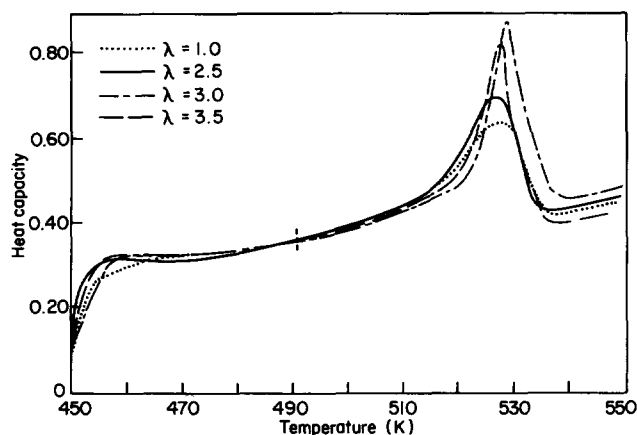


Figure 3 The effect of draw ratio  $\lambda$  on the melting endotherm of PET

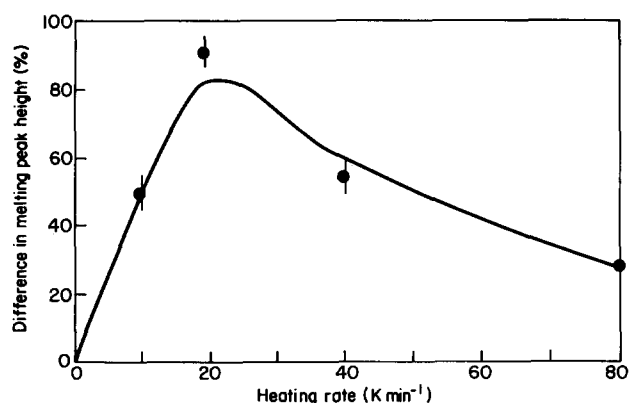


Figure 4 The percentage difference in melting peak height as a function of the d.s.c. heating rate between annealed samples 4A to 9A

effect was clearly kinetic, arising from melting occurring at rates comparable with relaxation of the strained melt, combined with thermal lag at high rates of heating.

The heat of fusion was found to be comparatively insensitive to draw ratio (see Table 1), and the relative heights of the melting endotherms, i.e. the maximum apparent specific heat, could be used as an indirect measure of orientation (see Figure 5). They exhibited the same dependence on  $\lambda$  as the Hermans function (see Figure 6), both reaching limiting values with  $\lambda$  values of 3.5. This somewhat limited their use to the characterization of samples with  $\lambda$  values below 3.5.

Within each type of oriented sample, annealed or unannealed, the degree of crystallinity, as determined from peak area, did not change with draw ratio but was dependent on the crystallization and annealing conditions.

The melting point, as defined by the temperature of the maximum rate of melting, changed progressively with draw ratio within each set of samples, and up to the limit used in the present study,  $\lambda = 5$  (see Figure 7).

Measurement of the melting characteristics of the PET samples to determine the peak melting temperature is a relatively rapid and simple experimental procedure. It did, however, give a more precise estimate of the draw ratio in commercially prepared samples than either the Hermans function, for the crystalline regions, or the melting peak height.

#### Effect of orientation on melting

The effect of draw ratio on the melting point is readily understood in terms of the increased entropy of the amorphous regions, and the decrease with slower rates of

heating in terms of relaxation of the deformed melt increasing with time. Progressive melting will decrease the melt viscosity, and hence increase mobility<sup>11</sup>.

The effect of equilibrium deformation on the melting temperature has been considered by Krigbaum and coworkers<sup>12-14</sup> in terms of Flory's treatment of elasticity<sup>15</sup>, and they have derived the relationship:

$$1/T_m = 1/T_m^\circ - R/N\Delta H_f [(6N/\pi)^{1/2}\lambda - (\lambda^2/2 + 1/\lambda)] \quad (3)$$

which relates the equilibrium melting points,  $T_m$  at  $\lambda$  and  $T_m^\circ$  at  $\lambda = 1$ , to the molar heat of fusion ( $\Delta H_f$ ) and number of statistical segments between entanglements ( $N$ ). Melting point  $T_m$  is inappropriate to the present measurements since it represents an equilibrium value obtained by extrapolation to eliminate crystal size effects. It is also difficult to be precise about the value of  $N$  except that it is likely to be about 100. This value implies an approximately linear dependence of the melting point on  $\lambda$ , as observed in Figure 7, but the intercept,  $T_m^\circ$ , is not the equilibrium value.

The increased melting point of deformed networks is assumed to be derived entirely from the decrease in configurational entropy on melting the crystals into an oriented rather than a randomly ordered melt. This difference in the entropy of the melt is:

$$-\Delta S_c = R/2N(\lambda^2 + 2/\lambda - 3) \quad (4)$$

where  $N$  is the number of base monomer units between entanglements.

For lamellar crystals of a monodisperse polymer, the melting has been related to the number of repeat units  $n$  in

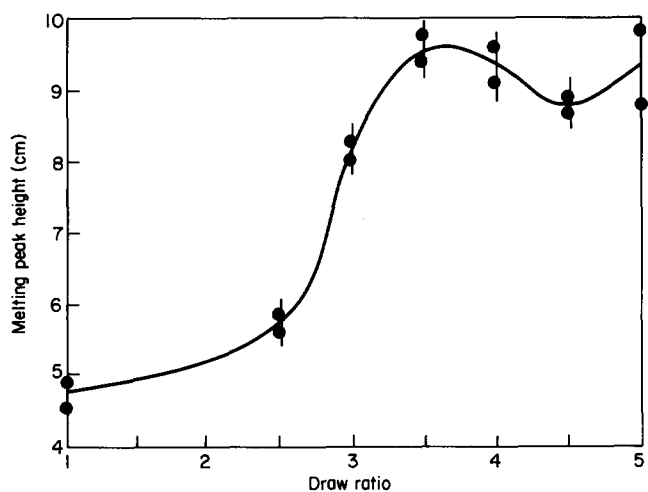


Figure 5 Melting peak height as a function of draw ratio for unannealed samples 4B to 9B

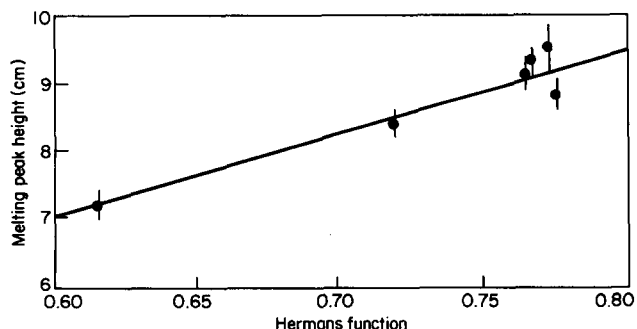


Figure 6 The relationship between melting peak height and the Hermans function for annealed samples 4A to 9A

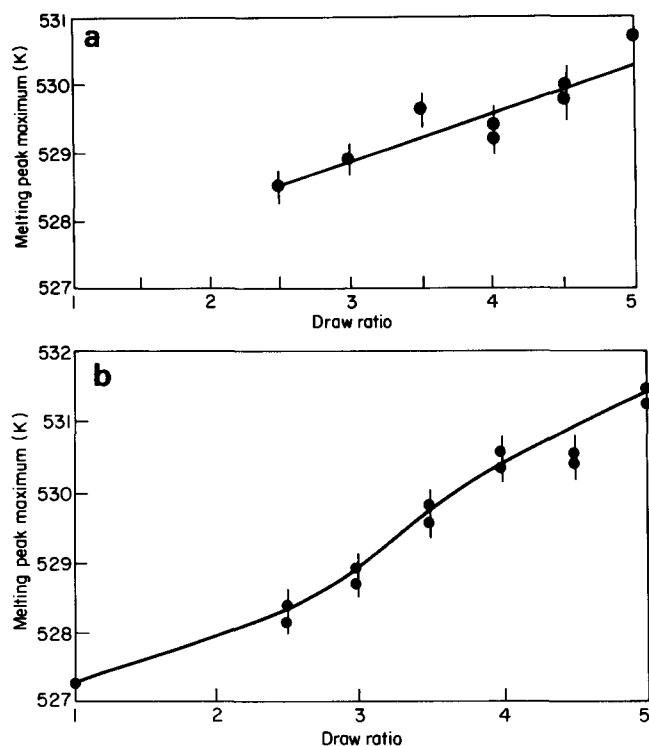


Figure 7 Melting peak temperature maxima as a function of draw ratio for (a) annealed samples 4A to 9A and (b) unannealed samples 4B to 9B

the thickness of the crystal<sup>16</sup>:

$$T_m = T_m^\circ [1 - 2RT_m \ln(n)/n\Delta H_f - 2\sigma/n\Delta H_f] \quad (5)$$

where  $\sigma$  is the lateral surface free energy. Introducing the additional entropy term gives:

$$T_m' = T_m^\circ [T_m^\circ \Delta S_f/n\Delta H_f + 1 - 2RT_m' \ln(n)/n\Delta H_f - 2\sigma/n\Delta H_f] \quad (6)$$

for the melting point of oriented material. Equating  $T_m$  with  $\lambda=1$ , and  $T_m'$  with all other values of  $\lambda$  then:

$$T_m' = T_m + (RT_m^\circ T_m'/2Nn\Delta H_f)(\lambda^2 + 2/\lambda - 3) \quad (7)$$

Equation (5) should be corrected for the polydispersity of the polymer, and chain folding<sup>17</sup>, but this does not alter the form of equation (6), merely the definition of  $T_m$ .

Accordingly equation (7) is considered to be more general than the simple model used to derive it. It can be applied to the present case of rapidly determined, non-equilibrium, melting points since the model is applicable to the melting of the lamellar crystals present within the specimens. The model adopted in deriving equation (7) is one in which the amorphous regions only are oriented. Since crystallization occurred on drawing amorphous material, the draw ratio of the amorphous region is identical to the macroscopic draw ratio  $\lambda$ . This would not have been the case if crystalline material had been cold-drawn. Allowance would then have been required for the hard crystalline regions not deforming. The draw ratio of the amorphous regions  $\lambda'$  is not the macroscopic draw ratio  $\lambda$ , but correcting for the degree of crystallinity  $\chi$  it is:

$$\lambda' = \lambda/(1 - \chi)$$

Application of equation (7) to the melting points presented in Figure 7 gave a reasonably linear dependence of  $T_m'$  on  $T_m'(\lambda'^2 + 2/\lambda' - 3)$  and an intercept of  $T_m$  consistent with that observed for the undeformed specimens (see Figure 8). The slope of  $3.5 \times 10^{-5}$ ,

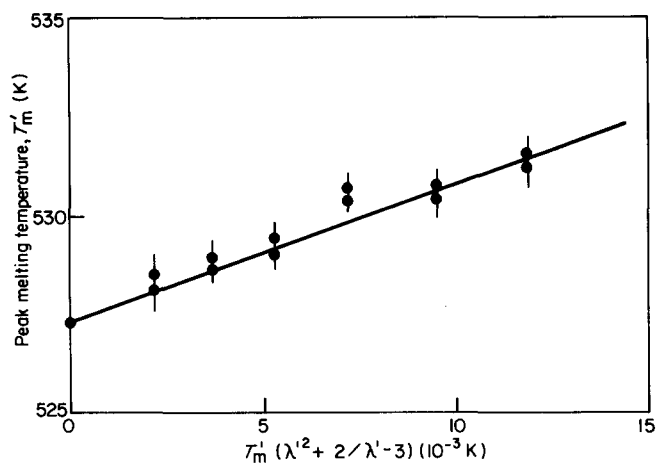


Figure 8 Orientation entropy function for unannealed samples

equivalent to  $RT_m^\circ/2\Delta H_f Nn$ , gave  $Nn \sim 120$ , using the following standards:  $T_m^\circ = 556 \text{ K}^{18}$  and  $\Delta H_f = 27 \text{ kJ mol}^{-1}$ .<sup>19</sup>

It is also inherent from the model that the ratio of  $n/N$  is equivalent to the ratio of crystalline to amorphous sequences and hence the crystalline/amorphous content. From the observed heat of fusion of the samples ( $\sim 45 \text{ J g}^{-1}$ ), this is 0.47. The value of  $N$  was accordingly about 16 and that of  $n$  was 7–8 repeat units. Values of  $n$  between 6 and 10 would be expected from the thickness of the crystals grown under these conditions. Accordingly the model accounts for the observed dependence of the melting point on draw ratio.

## CONCLUSIONS

D.s.c. can be used routinely to assess the relative orientation in PET provided that the samples have been given identical heat treatments. Samples with draw ratios above 3.5, which have similar crystalline orientation, as characterized by the Hermans function and by the height of the crystalline melting endotherm, can be separated by the measurement of the melting point at  $20 \text{ K min}^{-1}$ .

## REFERENCES

- 1 Aref-Azar, A., Biddlestone, F., Hay, J. N. and Haward, R. N. *Polymer* 1983, **24**, 1245
- 2 Casey, M. *Polymer* 1977, **18**, 1219
- 3 Prevorsek, D. C. *J. Polym. Sci.* 1971, **32**, 343
- 4 Prevorsek, D. C., Haque, P. J., Sharma, R. K. and Reimschuessel, R. C. *J. Macromol. Sci., Phys.* 1973, **138**, 127
- 5 Lemanska, G. and Narebska, A. *J. Polym. Sci., Polym. Phys. Edn.* 1980, **18**, 917
- 6 Linder, W. L. *Polymer* 1973, **14**, 9
- 7 Gupta, V. B. and Kumar, S. *Polymer* 1978, **19**, 953
- 8 Deopura, D. L., Kumar, V. and Sinha, T. B. *Polymer* 1977, **18**, 856
- 9 Dumbleton, J. H. and Bowles, B. B. *J. Polym. Sci., Polym. Phys. Edn.* 1966, **4**, 951
- 10 Blundell, D. J. and Osborn, B. N. *Polymer* 1983, **24**, 953
- 11 Wunderlich, B. 'Macromolecular Physics', Vol. 3, 'Crystal Melting', Academic Press, New York, 1980, p. 96
- 12 Krigbaum, W. R. and Roe, R. J. *J. Polym. Sci.* 1964, **A2**, 4391
- 13 Krigbaum, W. R., Dawkins, J. V., Via, G. H. and Balta, Y. I. *J. Polym. Sci., Polym. Phys. Edn.* 1966, **4**, 475
- 14 Krigbaum, W. R., Dawkins, J. V. and Via, G. H. *J. Polym. Sci., Polym. Phys. Edn.* 1969, **6**, 257
- 15 Flory, P. J. *J. Chem. Phys.* 1947, **15**, 397
- 16 Hay, J. N. *J. Polym. Sci., Polym. Chem. Edn.* 1976, **14**, 2845
- 17 Booth, C., Beech, D. R., Dodgson, D. V., Sharpe, R. R. and Waring, J. S. *Polymer* 1972, **13**, 73 and 246
- 18 Ikeda, M. *Kobunshi Kagaku* 1967, **24**, 378
- 19 Droscher, M. and Wegner, G. *Polymer* 1978, **19**, 43